Chapter 5

Effect of doping and surface charge on the antibacterial response of $Mg_{1-x}Ca_xSi_{1-x}Zr_xO_3$ (x = 0 - 0.4) bioceramics

This chapter discusses the effect of surface charge and co-substitution of Ca and Zr in $MgSiO_3$ [$Mg_{1-x}Ca_xSi_{1-x}Zr_xO_3$ (x = 0 - 0.1, 0.2, 0.3, 0.4); MCSZO-X, X=0 – 4] on their antibacterial response. The MCSZO-X bioceramics were synthesized using solid-state route. The influence of Ca and Zr co-doping on crystallite size of MCSZO-X has been analysed using X-ray peak profile analyses. The surface charges were developed by corona poling (30 min) of sintered MCSZO-X samples as well as HA samples at temperature and voltage of 500ºC and 20 kV, respectively. In addition, the antibacterial response of MCSZO-X ceramics was evaluated by measuring of reactive oxygen species (ROS), the levels of superoxide dismutase, catalase, and level of protein and lipid peroxide.

5.1. Crystalline Size and lattice strain analyses

The discs were optimally sintered at different temperatures like, MCSZO-0 at 1380 °C for 6 h, MCSZO- X (X = 1 – 3) at 1350°C for 3 h and MCSZO - 4 at 1320º C for 3 h. The XRD analyses of sintered MCSZO-X (X = 0 - 4) and HAP samples revealed the formation of pure phases with some minor peaks of $CaSiO_3$ and $CaMgSiO_3$ (JCPDS #19-0239) [1, 2]. The crystallite size and strain for MCSZO -X samples were calculated from the diffraction data using Scherrer, modified Scherrer (Figure. 5.1), size-strain plot (SSP) (Figure. 5.2) and Williamson-Hall (WH) plot (Figure. 5.3). The average crystal size and strain for MCSZO-X samples were computed [Table 5.1].

Figure. 5.4 represents the EDS spectra of MCSZO- X powder, which confirm the presence of Mg, Ca, Si, Zr and O ions.

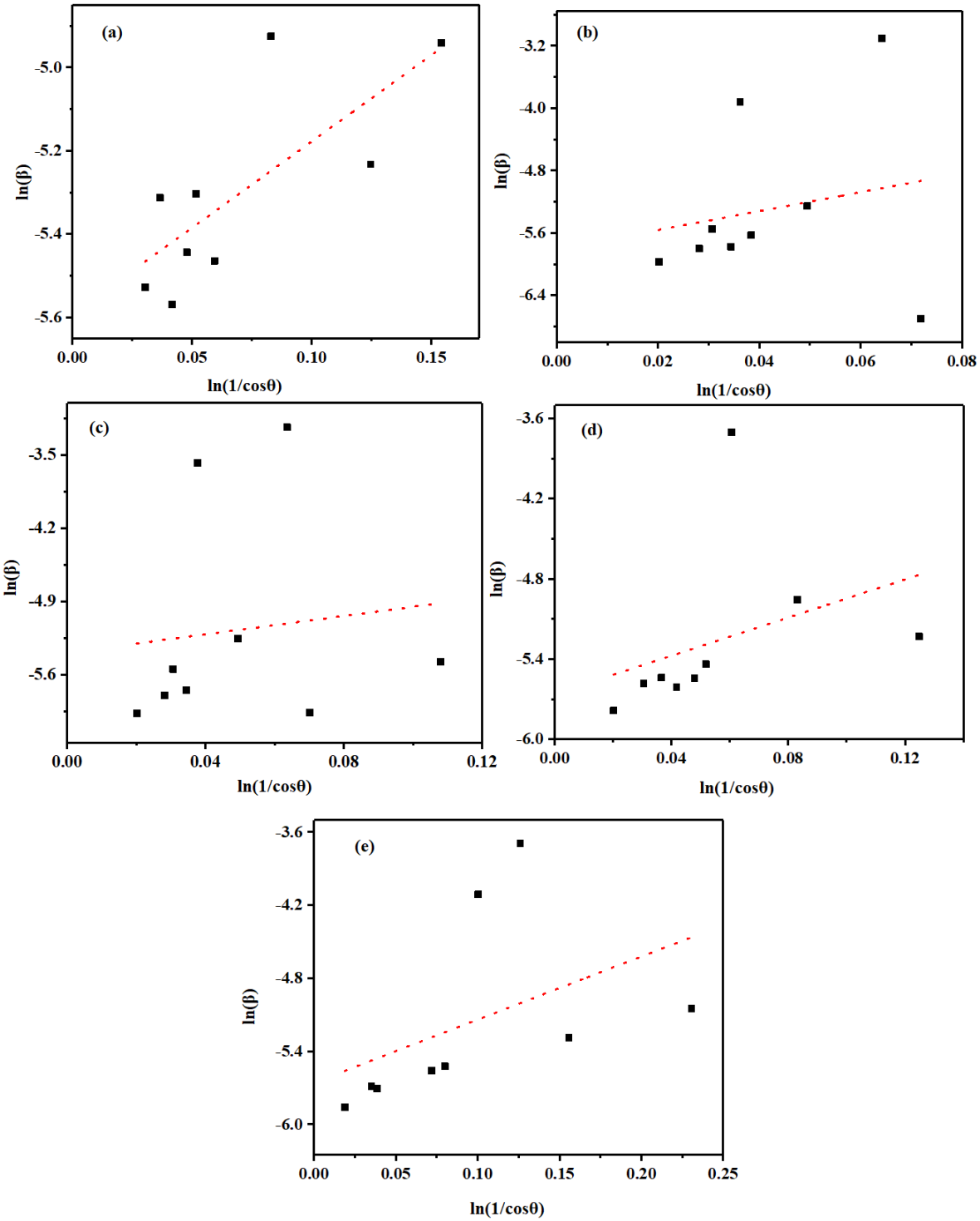

Figure 5.1. Modified Scherrer plots for MCSZO – X (X = 0 - 4) bioceramics. (a) X = 0, (b) X = 1, (c) X = 2, (d) X = 3, and (e) X = 4.

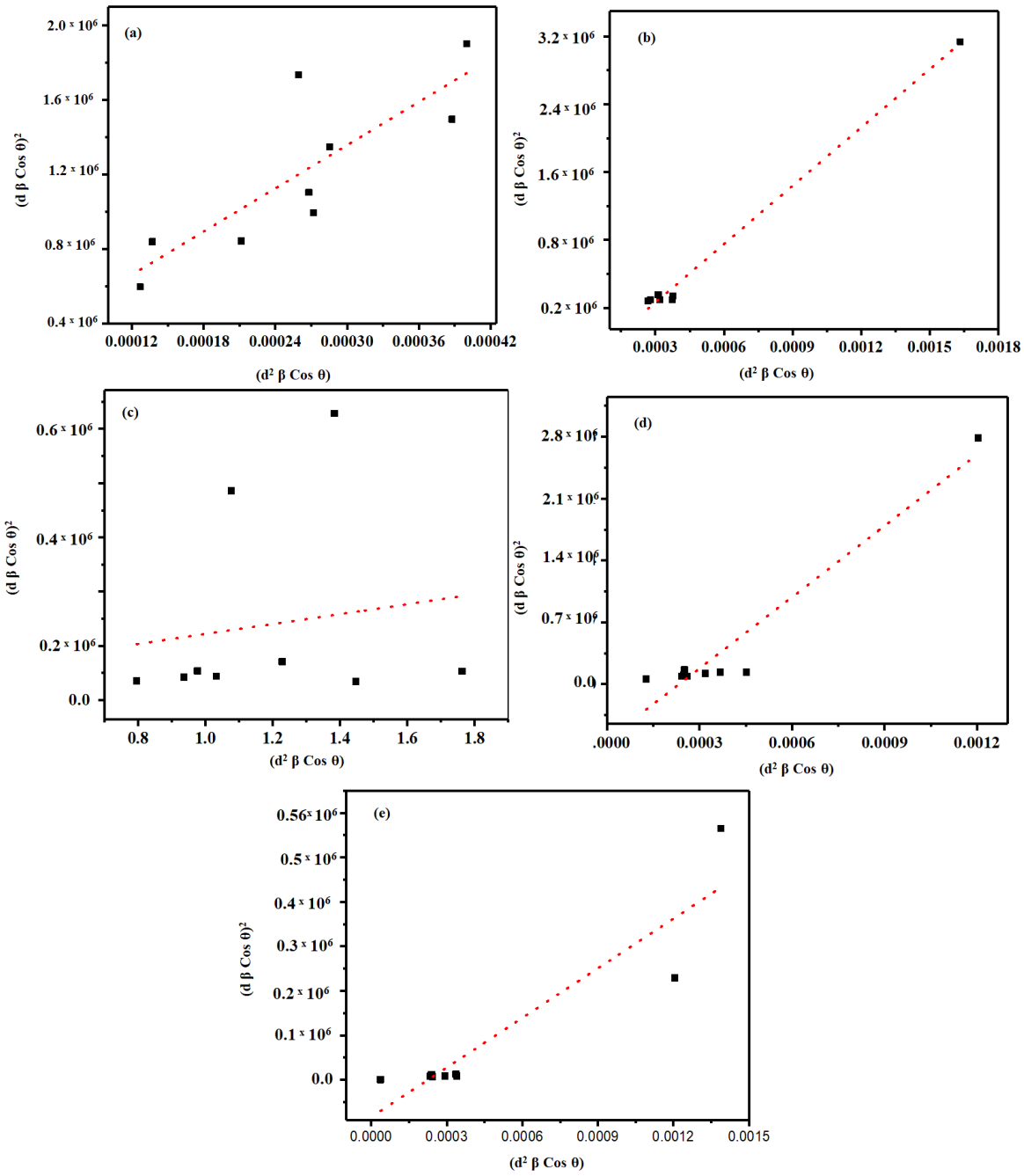

Figure 5.2. Size -strain plots for MCSZO – X (X = 0 -4) bioceramics. (a) X = 0, (b)X = 1, (c) X = 2, (d) X = 3 and (e) X = 4.

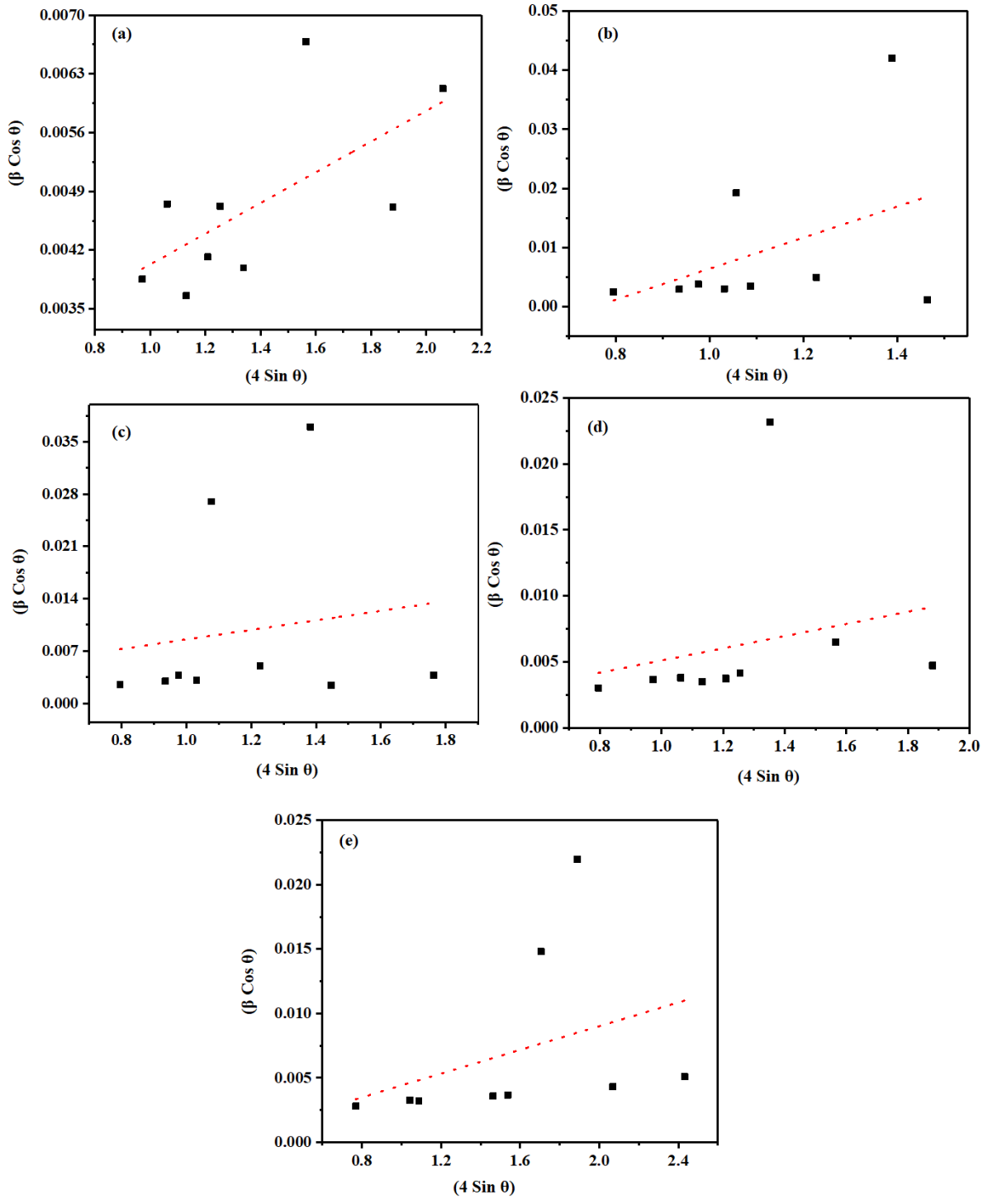

Figure 5.3. Williamson-Hall plots for MCSZO – X (X = 0 -4) bioceramics. (a) X = 0, (b)X = 1, (c) X = 2, (d) X = 3 and (e) X = 4.

Overall, the crystallite size, calculated from various approaches, (scherrer, modified Scherrer methods, W- H plot and SSP plot method), the SSP plot method offers more close values of size and strain as the high-intensity points are closer to the linear fit.

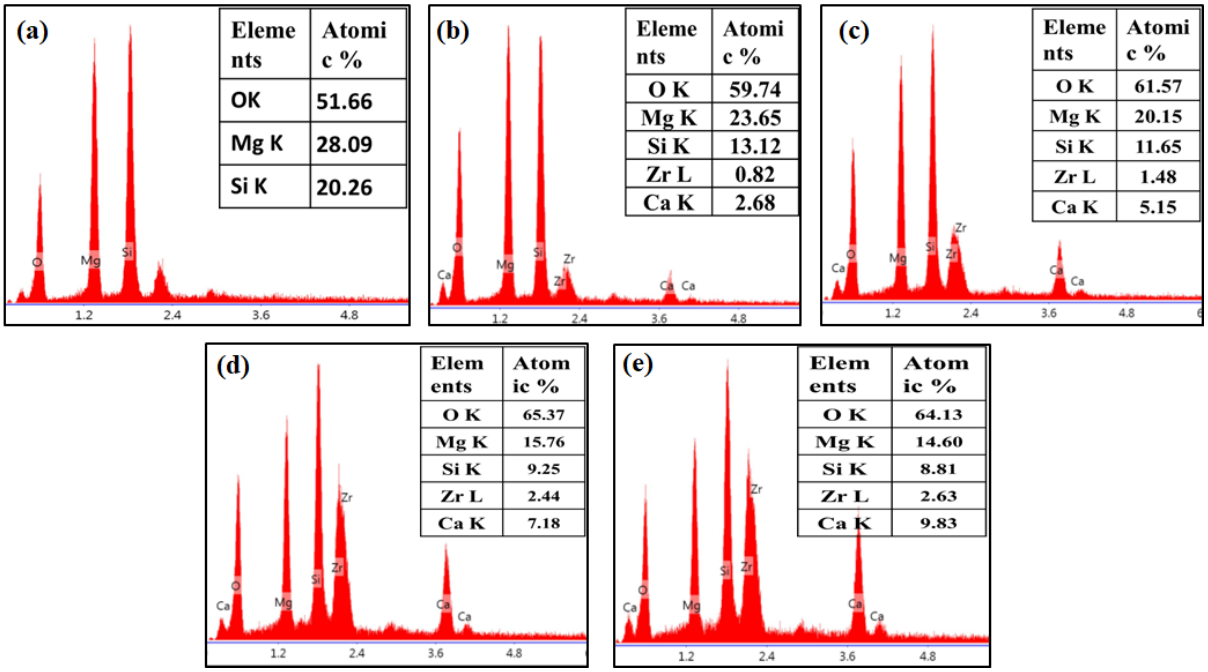

Figure 5.4. EDS spectrum of MCSZO-X (X = 0 – 4) powders. (a) X= 0, (b) X= 1, (c) X= 2, (d) X= 3, and (e) X= 4.

Table 5.1: The crystallite size and lattice strain for the developed MCSZO-X (X = 0 – 4) bioceramics using X-ray peak profile analyses.

	Methods	Samples				
		MCSZO-0	MCSZO-1	MCSZO-2	MCSZO-3	MCSZO-4
Crystallite size (D) in nm	Scherrer Method (nm)	38 ± 13.4	35 ± 6.8	36 ± 20.5	33 ± 12.4	34 ±17.3
	Modified Scherrer method (nm)	41	39	38	28	33
	Williamson-Hall plot (nm)	69	64	63	37	39
	Size-strain Plot (nm)	63	59	58	54	57
Lattice Strain (ε)	Williamson-Hall plot	3.7×10^{-3}	3.3×10^{-3}	3.2×10^{-3}	2.2×10^{-3}	2.9×10^{-3}
	Size-strain Plot	3.7×10^{-3}	3.3×10^{-3}	3.2×10^{-3}	2.2×10^{-3}	2.9×10^{-3}

5.2. Measurement of surface charge

Thermally stimulated depolarization current (TSDC) spectrum [Figure 5.5] was used to evaluate the charge, produced on the surface of MCSZO-X electret samples as [3],

$$Q = \frac{1}{\beta}\int I\,(T)dT \qquad (5.1)$$

Where β, T and I represent the heating rate, temperature and current, respectively. The surface charge densities, calculated for MCSZO-X electrets are 0.25, 0.29, 0.32, 0.17, 0.16 μC/cm^2, respectively.

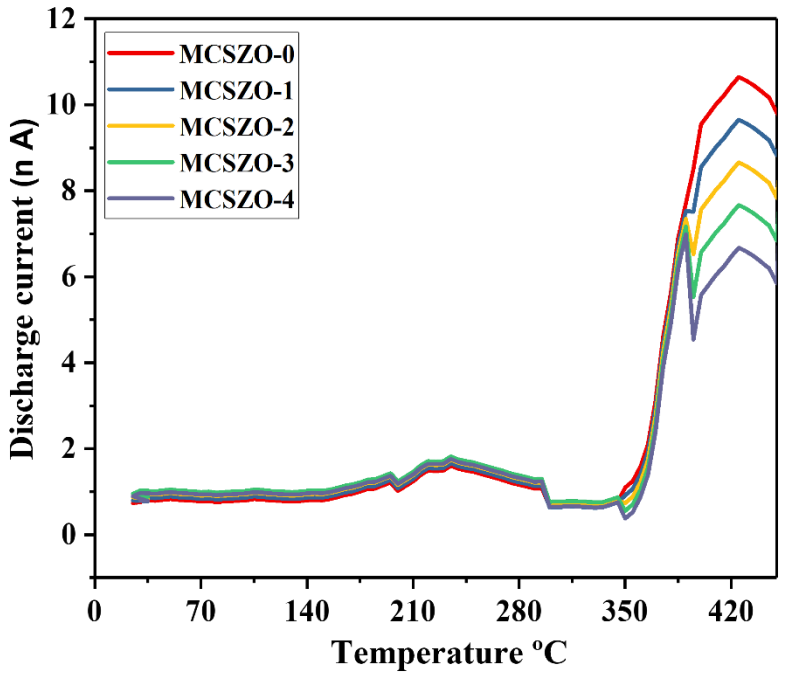

Figure 5.5. Thermally stimulated depolarization current (TSDC) plot for MCSZO-X (X = 0 – 4) electrets.

5.3. Antibacterial response

The in vitro antibacterial response of MCSZO-X (X= 0 - 4) electret samples were evaluated with *E. coli* and *S. aureus* bacteria. For this purpose, both, quantitative and qualitative analyses as follows.

5.3.1. Quantitative assessment

5.3.1.1. MTT assay

The results of MTT assay for both, *E. coli* and *S. aureus* bacteria, cultured on the surface of uncharged, MCSZO-X electrets and HA samples are shown in Figure. 5.6. The co-doping of Ca^{2+} and Zr^{4+} in $MgSiO_3$ increases the antibacterial response. In comparison to uncharged HA, statistical analyses demonstrate that all uncharged and MCSZO-X electrets exhibit significantly higher antibacterial responses.

The viability of both, *S. aureus* and *E. coli* bacteria on uncharged MCSZO-X samples are decreased by (14, 17, 23, 36, 35 %) and (16, 19, 25, 40, 39 %), respectively, in comparison to uncharged HA [Figure. 5.6 (a and b)]. However, negative end of MCSZO-X electrets decreased the bacterial viability of both, *S. aureus* and *E. coli* by (21, 22, 27, 39, 37 %) and (29, 37, 39, 51, 48 %) than the uncharged HA. The negative end of MCSZO-X electrets decreased the viability of *S. aureus* and *E. Coli* by (18, 20, 24, 37, 36 %) and (17, 27, 29, 44, 40 %) than negative end of HA electrets, respectively. However, negative end of HA electrets reduced the viability of *S. aureus* and *E. coli* by 3.17 % and 14.19 % as compared to their uncharged HAP samples, respectively. Although, positive end of MCSZO-X electrets decreased the viability of *S. aureus* and *E. coli* bacteria by (26, 33, 35, 46, 42.8 %), and (24, 25, 30, 43, 42.2 %), in comparison to positive end of HAP electrets, respectively. However, positive end of HAP electret samples decreased the viability of both, *S. aureus* and *E. coli* bacteria by 13 % and 4 % as compared to their uncharged HAP samples. This suggests that formation of electret enhances the antibacterial response.

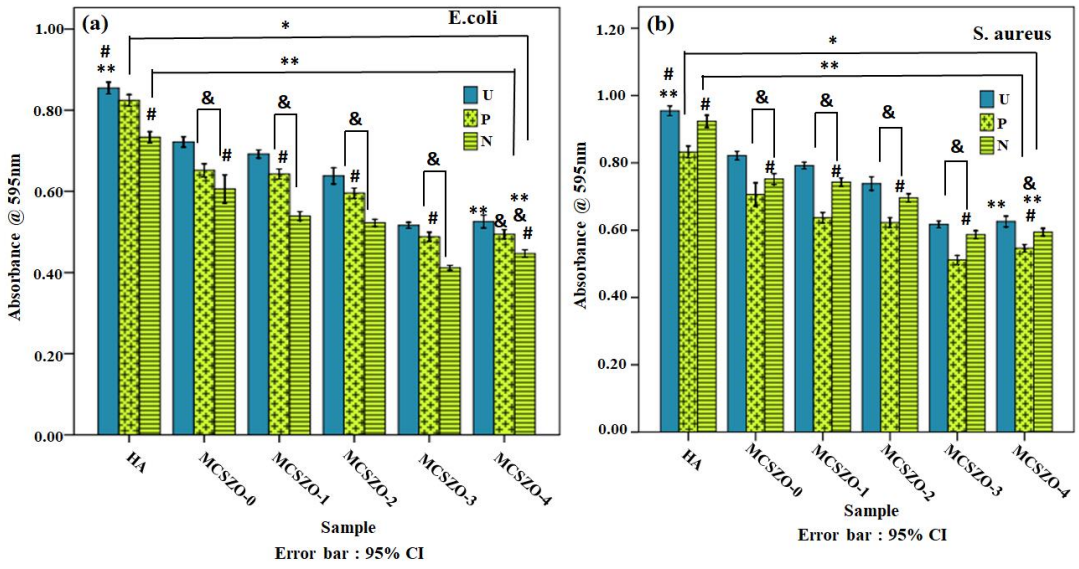

Figure 5.6. Optical density (OD) of E. coli (a) and S. aureus (b) bacteria towards uncharged, negative and positive ends of MCSZO-X (X = 0 - 4) electret surfaces and HAP control. (*) indicates statistically significant variation, at $p \leq 0.05$, among all MCSZO-X samples in comparison to uncharged HA. Similarly, (**) indicates statistically significant variation, at $p \leq 0.05$, among all MCSZO-X samples, as compared to the positive end of HA electret surfaces. (#) indicates statistically significant variation, at $p \leq 0.05$, among all MCSZO-X samples, compared to the negative end of HA electret surfaces. The (&) indicates the significant variation, at $p \leq 0.05$, among all the uncharged MCSZO-X samples, as compared to positive and negative end of MCSZO-X electret surfaces. (U- uncharged, P- Positive end of electrets, N- Negative end of electrets).

Figure. 5.7 shows the antibacterial ratio of *E. coli* and *S. aureus* bacteria on uncharged, MCSZO-X electrets and HA pellets. In the case of *E. coli* bacteria, antibacterial ratio is calculated to be (29, 33, 37, 50, 48 %), (37, 38, 42, 53, 52 %), and (40, 47, 49, 60, 57 %) on the uncharged, positive and negative ends of MCSZO-X electrets, respectively. Nevertheless, for the uncharged, positive and negative ends HA of electrets, it was 17 %, 19 %, and 28 %, respectively. However, the antibacterial ratio of *S. aureus* bacteria on the uncharged, positive

and negative ends of MCSZO-X electrets are (20, 23, 28, 40, 39 %), (30, 38, 39, 50, 47 %), (29, 28, 32, 43, 42 %), respectively, while it was only 7 %, 19 % and 10 % on the surfaces of uncharged, negative and positive ends of HA electrets. The results suggest that, the antibacterial ratios of the uncharged and MCSZO-X electrets are considerably higher than those of HAP samples, respectively, for both, *S. aureus* and *E. coli* bacteria.

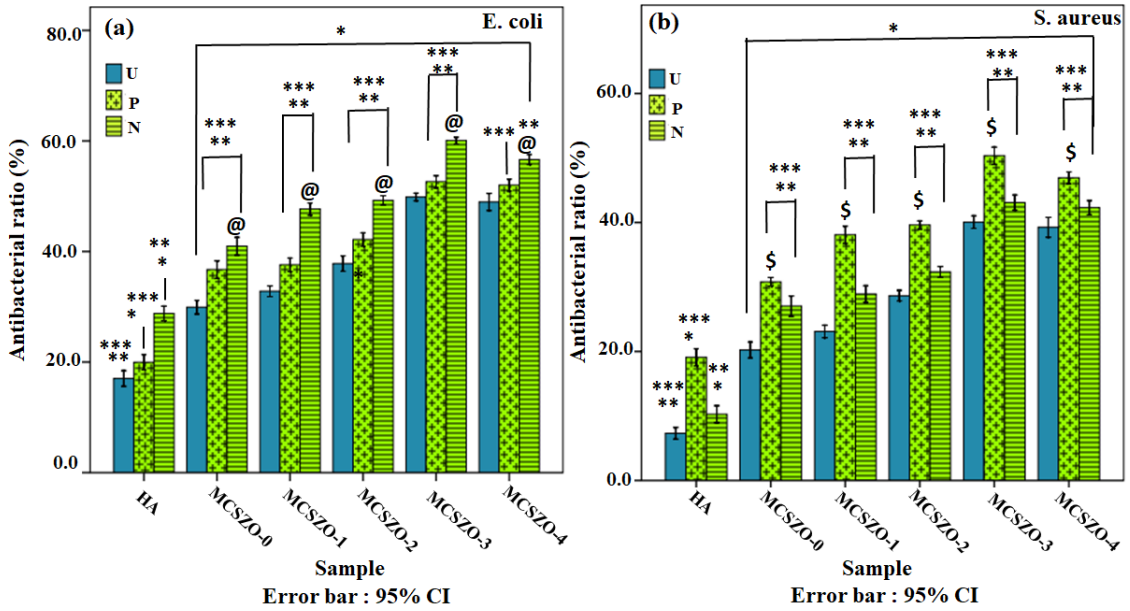

Figure 5.7. Antibacterial ratio for E. coli (a) and S. aureus (b) bacteria towards uncharged, negative and positive ends of MCSZO-X (X = 0 - 4) electret surfaces and HAP control. (*), (**) and (***) indicate significant variation among all the uncharged, positive and negative ends of MCSZO-X electret surfaces with those of HA, at $p \leq 0.05$, (@) indicates the significant variation in negative end of MCSZO-X electret surfaces with respect to their corresponding uncharged surfaces of MCSZO-X samples, at $p \leq 0.05$. ($) indicates the significant variation in positive end of MCSZO-X electret surfaces with respect to corresponding uncharged surfaces of MCSZO-X samples, at $p \leq 0.05$. (U- uncharged, P- Positive end of electrets, N- Negative end of electrets).

Overall, the MTT results demonstrate that the surfaces of MCSZO-X electrets reduce the bacterial adhesion by the action of electrostatic field. With increasing the concentration of Ca and Zr in MCSZO-X bioceramics, the antibacterial activity is observed to increase.

5.3.2. Qualitative assessment

5.3.2.1. Live/ dead assay

Figure. 5.8 and Figure. 5.9 demonstrates population of a live / dead bacterial cells, adhered on the surfaces of uncharged, MCSZO-X electrets and HAP samples, culture with both, *E. coli* and *S. aureus* bacteria. It is clearly seen that the population of *S. aureus and E. coli* bacteria on all the uncharged and MCSZO-X electrets represent higher number of dead bacterial cells in comparison to uncharged HA. The density of live bacteria is lower on the positive and negative ends of MCSZO-X electrets, in comparison to their uncharged MCSZO-X samples for *E. coli* [Figure. 5.8]. and *S. aureus* [Figure. 5.9]. The average number of the dead bacterial cells for S. aureus and *E. coli* was found to increase from about 45 to 70 and 25 to 60, respectively, with increasing the concentrations of Ca and Zr (X = 0 - 3) on positive electret surfaces of MCSZO-X sample. However, no significant change in number of dead bacterial cells was observed on further increasing the concentration of Ca and Zr from X = 3 to 4, which is in well agreement with MTT results. It has also been observed that with increase in the concentration of Ca and Zr from 0 to 0.3, the density of live bacterial cell decreases.

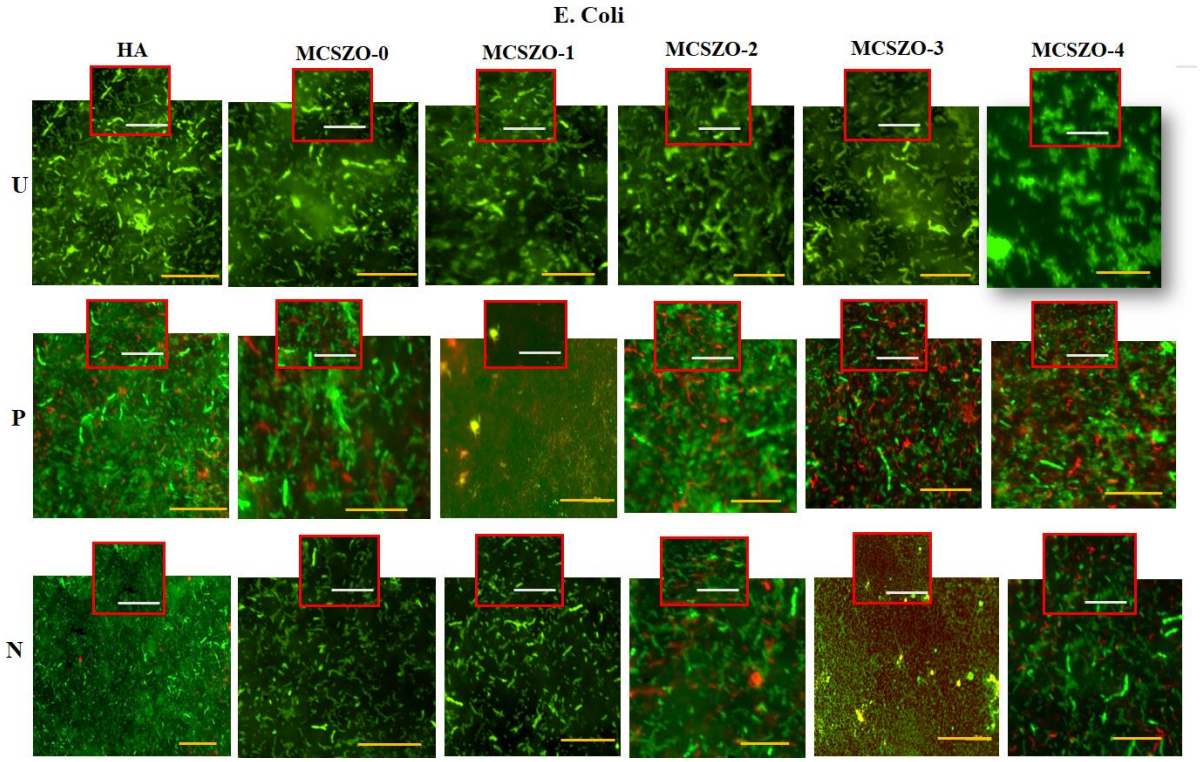

Figure 5.8. Fluorescence microscopy images, revealing the live and dead stain of E. coli bacteria, cultured towards uncharged, positive and negative ends of MCSZO -X (X = 0 – 4) electret surfaces as well as HA samples. (U- uncharged, P P-Positive end of electrets, N-Negative end of electrets, scale bar: 100 µm*).*

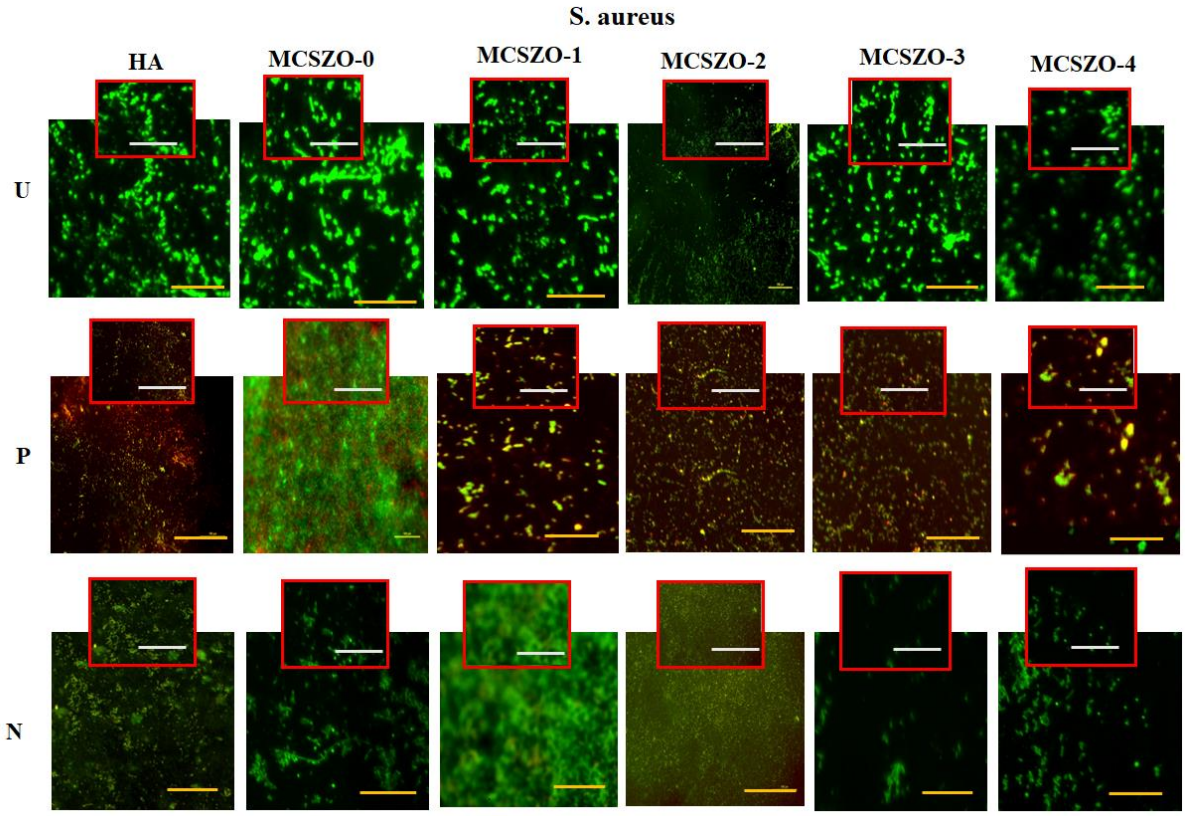

Figure 5.9. Fluorescence microscopy images, revealing the live and dead stain of S. aureus bacteria, cultured towards uncharged, positive and negative ends of MCSZO -X (X = 0 – 4) electret surfaces as well as HA samples. (U- uncharged, P P-Positive end of electrets, N-Negative end of electrets, scale bar: 100 µm*).*

5.4. Enzymatic activity

5.4.1. Super oxide dismutase (SOD) assessment

Figure. 5.10 represents the production of superoxide on the surfaces of uncharged, positive, negative ends of MCSZO-X electrets and HA samples, cultured with both, *E. coli* and *S. aureus* bacteria. It can be clearly seen that the production of O_2^- is lower on the surfaces of uncharged, negative end of MCSZO-X and HA electret samples as compared to positive end of MCSZO-X electrets and HA samples.

The formation of superoxide ion on the uncharged, positive and negative ends of MCSZO-X electrets, while cultured with *E. coli* bacteria, are (153, 160, 173, 185, 179 %), (234, 269, 288, 331, 326 %), and (168, 180, 187, 206, 200 %), respectively, as compared to uncharged HA. On the other hand, for *S. aureus* seeded surfaces of uncharged, positive and negative ends of MCSZO-X electret samples, the formation of superoxide ion is (141, 147, 153, 164, 155 %), (202, 224, 243, 273, 270 %), and (153, 162, 167, 18, 176 %), respectively, as compared to uncharged HA. It was suggested that after polarisation, the electrostatic surface charge generate an electric field, which promotes ROS formation [4]. According to reports, the proteins, DNA, and lipids, of bacterial cells are damaged by ROS (H_2O_2, O_2^-, OH, etc.) [5-8].

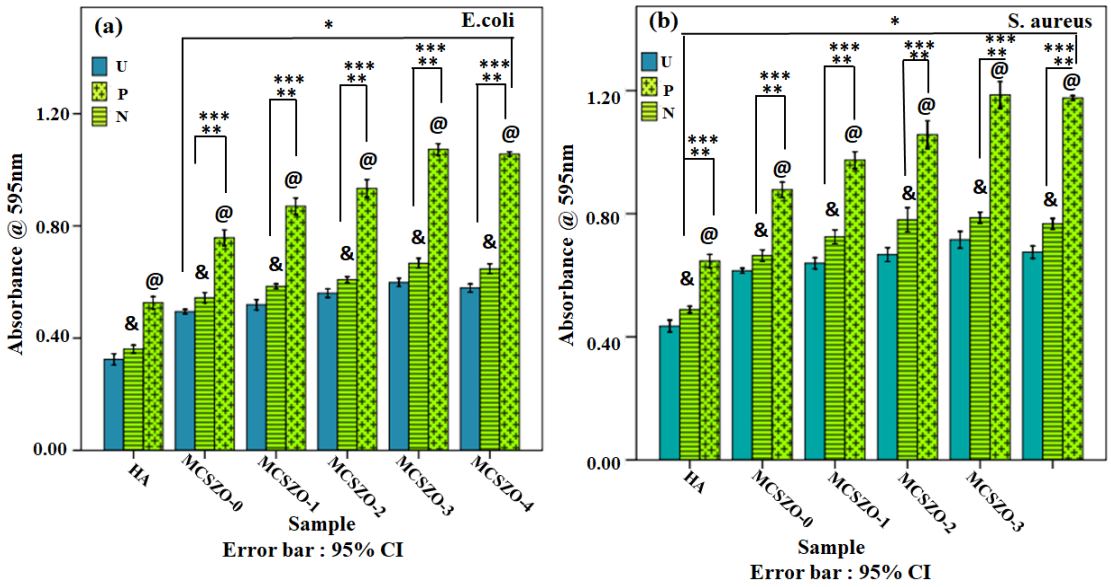

Figure 5.10. The content of superoxide ($^{\bullet}O_2^-$) for E. coli (a) and S. aureus (b) bacteria towards uncharged, negative and positive ends of MCSZO-X (X = 0 - 4) electret surfaces and HA control. (*), (**) and (***) represent statistically significant variation observed among all the uncharged, positive, and negative ends of MCSZO-X electret surfaces, as compared to the uncharged, positive, and negative ends of HA electret surfaces, respectively, at $p \leq 0.05$. (@) indicates statistically significant variation observed in negative end of MCSZO-X

electret surfaces, as compared to their uncharged counterparts, at $p \leq 0.05$. (&) indicates statistically significant variation, observed on the positive end of MCSZO-X electret surfaces, as compared to their uncharged counterparts, at $p \leq 0.05$. (U- uncharged, P-Positive end of electrets, N- Negative end of electrets).

5.4.2. Catalase assessment

Figure. 5.11 shows the catalase activity for *E. coli* and *S. aureus* bacteria, cultured with uncharged, positive, negative ends of MCSZO-X electrets and HA samples. The catalase activity demonstrates the time-dependent nature of H_2O_2 dissociation. In comparison to uncharged, positive and negative ends of HA samples, the surface of uncharged, positive and negative ends of MCSZO-X electrets bioceramics exhibit substantial reductions in catalase activity. Additionally, the statistical analyses furthermore demonstrate that positive end of MCSZO-X electret and HA samples have significantly lowered the catalase activity than uncharged and negative end of MCSZO-X electrets and HAP [Figure. 5.10. (a, b)].

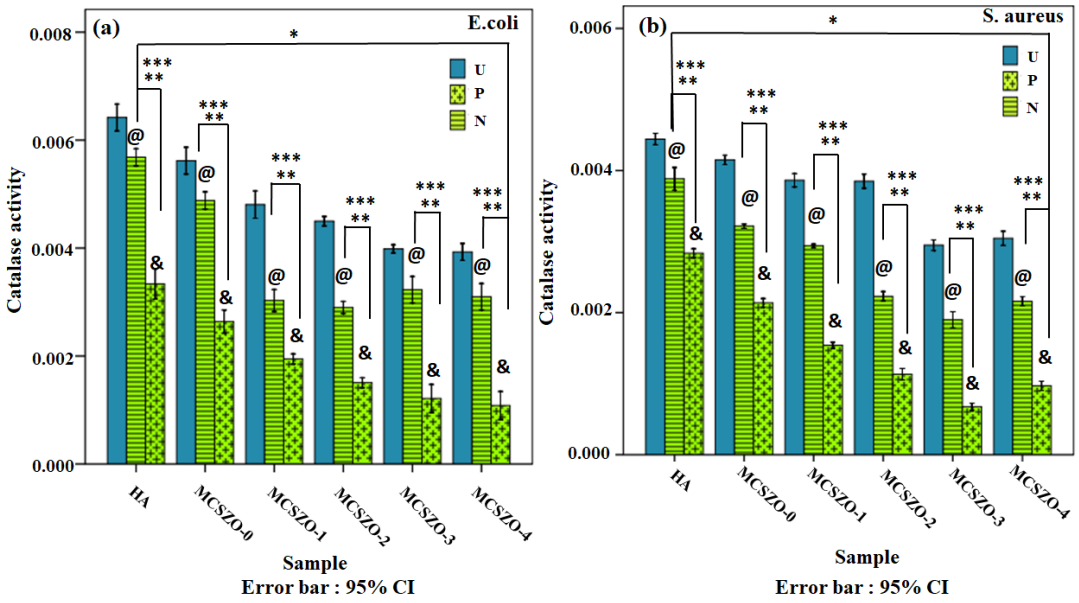

Figure 5.11. Catalase activity for E. coli (a) and S. aureus (b) bacteria towards uncharged, negative and positive ends of MCSZO-X (X = 0 - 4) electret surfaces and HAP control. (*), (**) and (***) indicate significant variation among all the uncharged, positive and negative ends of MCSZO-X electret surfaces with respect to those of HAP, at p ≤ 0.05, (@) indicates significant variation in negative end of MCSZO-X electret surfaces, as compared to their uncharged counterparts, at p ≤ 0.05. (&) indicates significant variation in positive end of MCSZO-X electret surfaces, as compared to their uncharged counterpart, at p ≤ 0.05. (U-uncharged, P-Positive end of electrets, N- Negative end of electrets).

The catalase activity on the surface of uncharged, negative and positive ends of MCSZO-X electrets, are (88, 75, 70, 62, 61 %), (76, 47, 45, 50, 48 %) and (41, 30, 23, 19, 17%) as compared to uncharged HA, respectively, while cultured with *E. coli* bacteria. Also, the catalase activity on the surface of uncharged, negative and positive ends of MCSZO-X electrets, are (93, 87, 88, 66, 68 %), (72, 66, 50, 42, 49 %) and (48 35, 26, 16, 22%) as compared to uncharged HA, respectively, while cultured with *S. aureus* bacteria. However, significant decrease in catalase activity has been observed on the positive end of MCSZO-X electrets for both, *E. coli* and *S. aureus* bacteria i.e., (41, 30, 23, 19, 17 %) and (48, 35, 26,

16, 21 %) respectively, in comparison to uncharged HA. It has been suggested that the decrease in catalase activity represents a slower dissociation of H_2O_2, resulting in the prolonged presence of reactive H_2O_2, which is toxic to bacterial cells [9-11].

5.4.3. Evaluation of protein concentration

Figure. 5.12 demonstrates the protein level for *E. coli* and *S. aureus* bacteria, while cultured with uncharged, positive, negative ends of MCSZO-X electrets and HA samples. The concentrations of protein have been observed to be lower on the surface of uncharged, positive, negative ends of MCSZO-X electrets, as compared to HA samples. In MCSZO-X electret samples, the amounts of *S. aureus* bacterial protein leakage from uncharged, positive and negative ends of electrets are (137, 151, 171, 202, 201 %), (241, 268, 283, 341, 350 %), and (160, 179, 196, 240, 231 %), respectively. However, it was 203 % and 114 % on positive and negative ends of HA electret samples, as compared to uncharged HA. Also, the amounts of damaged protein from the uncharged, positive and negative ends of MCSZO-X electrets, are (128, 154, 142, 175, 1880 %), (214, 229, 238, 292, 285 %), and (145, 166, 179, 210, 195 %), respectively, in comparison to uncharged HA, for *E. coli* bacteria. However, it was 170 % and 112 % on surfaces of the positive and negative ends of HA electrets. The decrease in protein concentration indicates that free radicals damage the cell walls. It is evident that the concentration of protein decreases on surface of positive end of electret in comparison to it's negative end and uncharged surface for both, *S. aureus* and *E. coli* bacteria, which indicates the percentage of higher number of free radicals on positive end of MCSZO-X and HA electrets. Overall, this result also demonstrates the bacterial damaged induced by ROS on the surface of positive end of MCSZO-X electret samples, which is significantly higher on the x = 0. 3 and x = 0. 4 samples. (i.e., higher Ca and Zr contents).

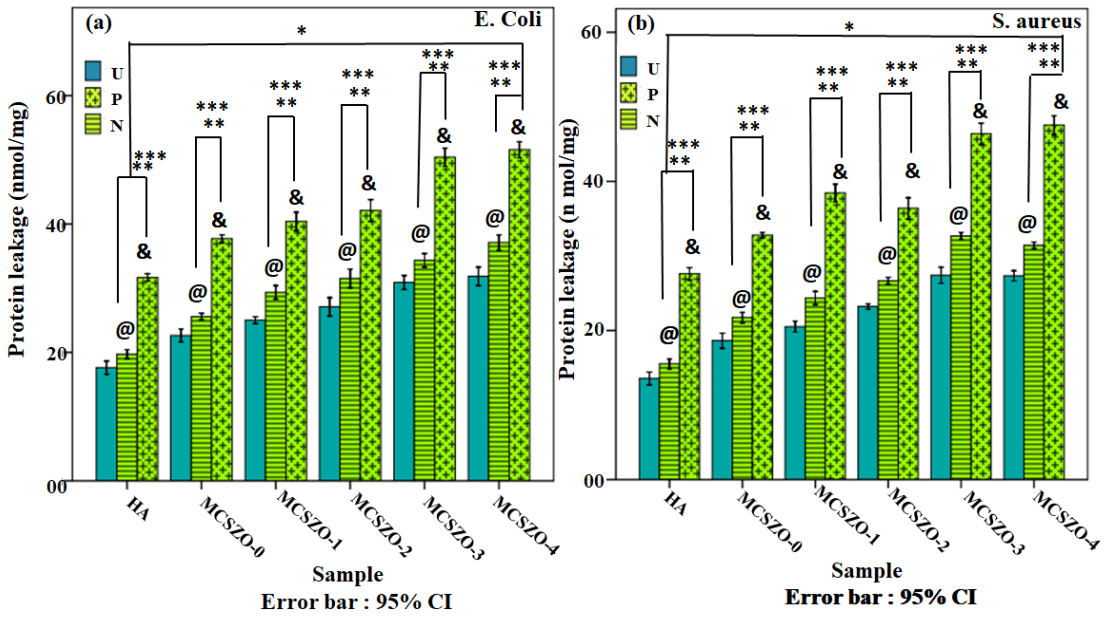

Figure 5.12. Protein leakage for E. coli (a) and S. aureus (b) bacteria towards uncharged, negative and positive ends of MCSZO-X (X = 0 - 4) electret surfaces and HA control. (*), (**) and (***) indicate significant variation among all the uncharged, positive and negative ends of MCSZO-X electret surfaces with respect to those of HA surfaces, at p ≤ 0.05, (@) indicates significant variation in negative end of MCSZO-X electret surfaces, as compared to their uncharged counterparts, at p ≤ 0.05. (&) indicates significant variation in positive end of MCSZO-X electret surfaces, as compared to their uncharged counterparts, at p ≤ 0.05. (U-uncharged, P-Positive end of electrets, N- Negative end of electrets).

5.4.4. Lipid peroxidation (LPO) assessment

Figure. 5.13 shows the content of MDA on uncharged, positive, negative ends of MCSZO-X electrets and HA pellets, cultured with both, *S. aureus* and *E. coli* bacteria. The production of ROS closely related to the MDA level [12]. According to statistical analyses, *S. aureus* and *E. coli* bacteria exhibit significantly higher MDA concentrations on uncharged, positive and negative ends of MCSZO-X electrets sample, than on uncharged, positive and negative ends of HAP electrets, respectively [Figure. 5.13 (a, b)]. The MDA concentration was found to be (126, 152, 163, 249, 233%), (233, 281, 290, 445, 444%), and (157, 175, 204, 298, 295%) on

the uncharged, positive, and negative ends surfaces of MCSZO-X electrets, respectively, while cultured with *S. aureus* bacteria. However, the MDA concentration for negative and positive ends of HAP electrets are (210 % and 302 %), respectively, as compared to uncharged HA.

Likewise, for *E. coli* bacteria, the MDA concentration has been calculated to be (152, 174, 209, 284, 273 %), (349, 405, 504, 679, 668 %) and (255, 256 292, 322, 308 %) on the uncharged, positive and negative ends of MCSZO-X electrets, respectively. However, the MDA concentration for positive and negative ends of HA electret are (302% and 302 %), respectively, in comparison as uncharged HA.

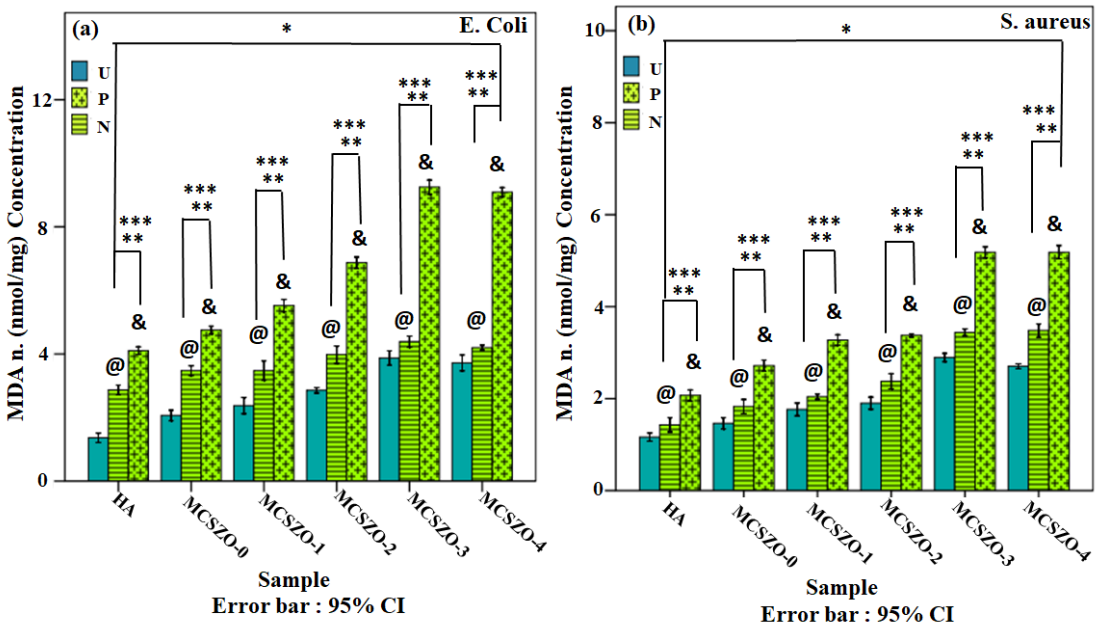

Figure 5.13. Concentration of MDA for E. coli (a) and S. aureus (b) bacteria towards uncharged, negative and positive ends of MCSZO-X (X = 0 - 4) electret surfaces and HA control. (*), (**) and (***) indicate significant variation among all the uncharged, positive and negative ends of MCSZO-X electret surfaces as compared to those of HA, at $p \leq 0.05$, (@) indicates significant variation in negative end of MCSZO-X electret surfaces, as compared to their uncharged counterparts, at $p \leq 0.05$. (&) indicates significant variation in positive end of MCSZO-X electret surfaces, as compared to their uncharged counterparts, at $p \leq 0.05$. (U- uncharged, P-Positive end of electrets, N- Negative end of electrets).

5.5. Discussion

Overall, the key findings show that the antibacterial activity of MCSZO-X (X = 0 - 4) bioceramics are influenced by number of factors, including the bacterial type, surface charge polarity, and doping of Ca^{2+} and Zr^{4+}. From X-ray peak profile analyses, it has been confirmed that with increasing the concentration of Ca and Zr from 0.1 to 0.3 in $MgSiO_3$ bioceramics, the crystallite size decreases from 38 - 33, 41 - 28, 69 - 37 and 63 - 54, as calculated from Scherrer, modified Scherrer, WH and SSP plots. Whereas, for the

concentration of Ca and Zr from 0.3 to 0.4, the crystallite size increases from 33 - 34, 28 - 33, 37 - 29 and 54 - 57 nm. Moreover, these changes appear due to the lattice contraction and distortion in $MgSiO_3$ ceramics. It has been revealed that the generation of oxygen vacancies decreases the crystallite size [13]. Consequently, the reduction in crystallite size, in the compositional range 0.1 to 0.3, can also be attributed to an increase in oxygen vacancy [Table 5.1]. Moreover, the present study also demonstrated that decrease crystallite size shows an increase in antibacterial properties.

The average number of the dead bacterial cells for S. aureus and E. coli was found to increase from about 45 to 70 and 25 to 60, respectively, with increasing the concentrations of Ca and Zr (X = 0 - 3) on positive electret surfaces of MCSZO-X sample. However, no significant change in number of dead bacterial cells was observed on further increasing the concentration of Ca and Zr from X = 3 to 4, which is in well agreement with MTT results.

It has been examined that the positive end of MCSZO-X electrets shows a higher amount of ROS such as superoxide and lipid peroxidation [Figure. 5.10 and Figure. 5.13] in comparison to their uncharged, negative end of MCSZO-X electrets as well as uncharged and HA electret samples. The formation of superoxide ion on the uncharged, positive and negative ends of MCSZO-X electrets, was increased with increasing the concentration of Ca and Zr from 0 to 3. While on increasing the concentration of Ca and Zr from 3 to 4, the formation of superoxide ion decreases, respectively for both E. coli and S. aureus bacteria [Figure 5.10].

The catalase activity is also lower on the positive end of MCSZO-X electrets in comparison to their uncharged and negative end MCSZO-X electret surfaces as well as uncharged and HA electrets [Figure. 5.11]. The positive end of MCSZO-X electrets demonstrates larger number of dead bacterial cell due to the higher concentration of ROS generation which damaged the DNA, and proteins of bacterial cells [14]. It has also been observed that the leakage of bacterial proteins is considerably more on the positive end of MCSZO-X electrets,

in comparison to their corresponding uncharged and negative end of HA electret samples [Figure. 5.12] which indicate that the positive end of electret surfaces leads to the remarkable higher destruction in the cytoplasmic component of bacterial cell [Figure. 5.14].

The bilayered structure of *E. coli* bacteria, which has a layer of peptidoglycan on the inside and a layer of lipopolysaccharides on the outside, making it more negative than *S. aureus* [15]. The negative charge on the bacterial membranes can be countered by the positive charge on the implant surface, which changes the structure of the lipid layer and increases the permeability of bacterial membrane. This causes the disintegration which, consequently, kill the cell membranes [Figure. 5.14][16, 17]. In an earlier study, it has been reported that the negative charge on the bacterial membrane is depolarized by the positive charged surfaces [18]. It induces cell death by altering the permeability of cellular membrane, which allows intracellular substances including glucose, proteins, and nucleic acids to flow out [18]. Additionally, because of electrostatic repulsion between negatively charged membrane of *E. coli* and negative end of electret surface, less number of bacterial cells was observed on the negative end of surfaces of MCSZO-X electret samples in comparison to positive end of MCSZO-X electrets and uncharged MCSZO-X samples [18, 19]. The negatively charged surface exhibited remarkable hydrophilicity, which decreases the bacterial cell population [20-23]. It has been reported that with the electrostatic repulsion, the hydrophilicity also plays an important role to enhance the antibacterial response [19, 20, 22, 24]. The charged surfaces generate a small electric field at the microscopic level and positive charged surfaces tend to produce higher levels of ROS such as OH^-, O_2^-, and H_2O_2, which kill the bacterial cells [5, 25]. In addition, Ca and Zr ions also promote ROS generation [26, 27]. Excessive oxidative stress can damage bacterial cell membranes as well as intracellular components such as, DNA and proteins, ultimately leading to cell death [Figure. 5.14][28].

From the above-mentioned observations, it has been suggested that with increasing the concentration of both, Ca^{2+} and Zr^{4+} in MCSZO-X (X = 0 – 4), antibacterial properties of prepared biocermics were enhanced.

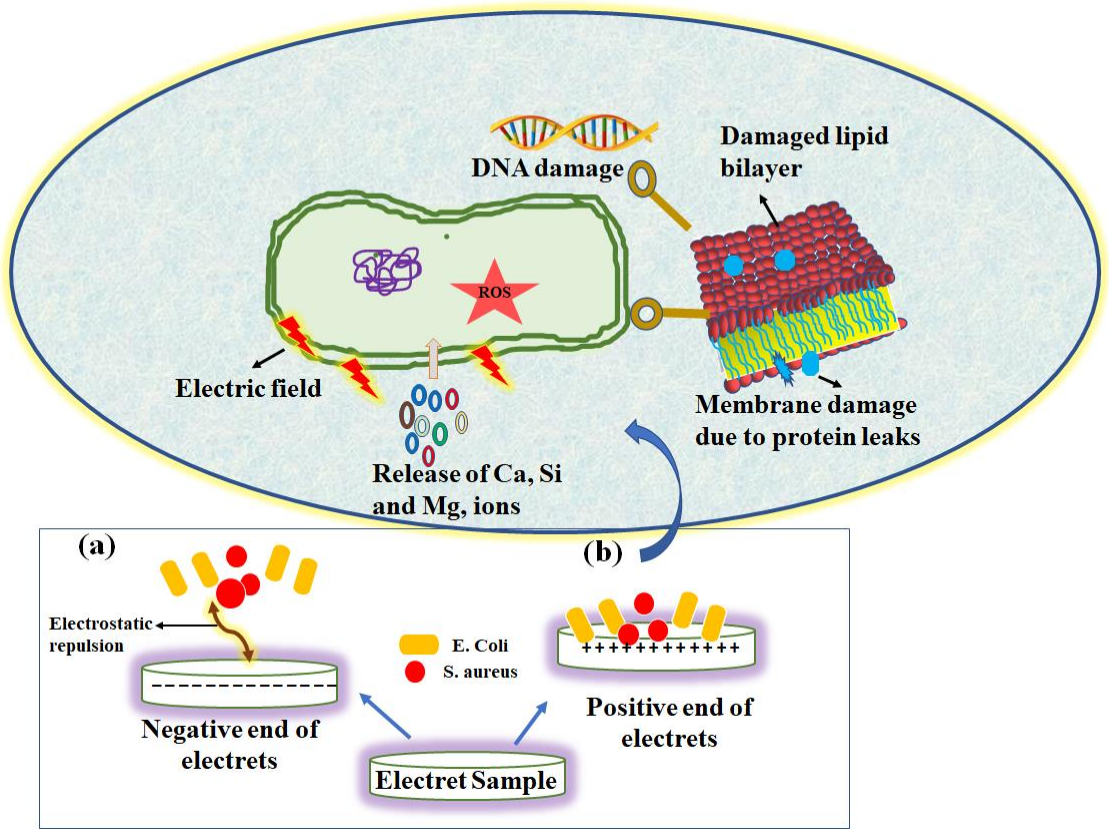

Figure 5.14. Schematic illustrating the mechanism of antibacterial response of negative (a) and positive (b) ends of electrets of MCSZO-X (X = 0 – 4) samples. (a) The electrostatic repulsion between negative end of electret and negatively charged bacterial membrane prevent the adhesion of bacteria (b) Production of reactive oxygen species (ROS) on the positive end of electret kill the bacterial cells by means of DNA damage, lipid layer distraction, membrane rupture [idea adapted from ref. 23].

5.5. Closure

Pure and Ca^{2+} and Zr^{2+} co-doped MCSZO-X (X = 0 - 4) bioceramics were developed by solid state synthesis route. From X- ray peck profile analyses reveal that the value of crystallite size and lattice strain decreases for the composition, X = 0 to X = 3 which again decreases for

X = 3 to X = 4, as calculated from WH and SSP methods. MTT results suggested that the viability of both, *S. aureus* and *E. coli* bacteria, are decreased by (14, 17, 23, 36, 35 %) and (16, 19, 25, 40, 39 %), respectively, on uncharged surfaces of MCSZO-X samples in comparison to uncharged HA. Further, negative end of MCSZO-X electrets demonstrate reduction in bacterial viability of both, *S. aureus* and *E. coli* by (21, 22, 27, 39, 37 %) and (29, 37, 39, 51, 48 %) than the uncharged HA. Also, positive end of MCSZO-X electrets shows the decrease in bacterial viability of *S. aureus* and *E. coli* bacteria by (26, 33, 35, 46, 42 %), and (24, 25, 30, 43, 42 %) respectively, in comparison to positive end HA electrets. In addition, the density of dead cell was higher on the surfaces of MCSZO-X electrets in comparison to their uncharged surfaces of MCSZO-X samples which confirm that surface polarization improves the antibacterial activity. Also, the from enzymatic activity results suggested that the positive end of MCSZO-X electrets, demonstrates higher number of dead bacteria cells in comparison to uncharged and negative end of MCSZO-X electrets. Overall, it has been confirmed that with increasing the concentration of Ca^{2+} and Zr^{4+} in MCSZO -X electrets, the antibacterial response enhances.

Bibliography

[1] Song M E, Kim J S, Joung M R, Nahm S, Kim Y S, Paik J H and Choi B H 2008 Synthesis and microwave dielectric properties of MgSiO3 ceramics *Journal of the American ceramic Society* **91** 2747-50

[2] Kanzaki M and Xue X 2017 Protoenstatite in MgSiO3 samples prepared by conventional solid state reaction *Journal of Mineralogical and Petrological Sciences* **112** 359-64

[3] Dubey A K, Yamada H and Kakimoto K-i 2013 Space charge polarization induced augmented in vitro bioactivity of piezoelectric (Na, K) NbO3 *Journal of Applied Physics* **114**

[4] Serena E, Figallo E, Tandon N, Cannizzaro C, Gerecht S, Elvassore N and Vunjak-Novakovic G 2009 Electrical stimulation of human embryonic stem cells: cardiac differentiation and the generation of reactive oxygen species *Experimental cell research* **315** 3611-9

[5] Tan G, Wang S, Zhu Y, Zhou L, Yu P, Wang X, He T, Chen J, Mao C and Ning C 2016 Surface-selective preferential production of reactive oxygen species on piezoelectric ceramics for bacterial killing *ACS applied materials & interfaces* **8** 24306-9

[6] Belenky P, Jonathan D Y, Porter C B, Cohen N R, Lobritz M A, Ferrante T, Jain S, Korry B J, Schwarz E G and Walker G C 2015 Bactericidal antibiotics induce toxic metabolic perturbations that lead to cellular damage *Cell reports* **13** 968-80

[7] Murphy M P, Holmgren A, Larsson N-G, Halliwell B, Chang C J, Kalyanaraman B, Rhee S G, Thornalley P J, Partridge L and Gems D 2011 Unraveling the biological roles of reactive oxygen species *Cell metabolism* **13** 361-6

[8] Chen X, Tian X, Shin I and Yoon J 2011 Fluorescent and luminescent probes for detection of reactive oxygen and nitrogen species *Chemical Society Reviews* **40** 4783-804

[9] Aebi H and Suter H 1966 On the peroxide sensitivity of acatalasie erythrocytes *Humangenetik* **2** 328-43

[10] Shin S-Y and Park J-H 1997 Activities of oxidative enzymes related with oxygen tolerance in Bifidobacterium sp *Journal of Microbiology and Biotechnology* **7** 356-9

[11] Gregory E M and Fanning D D 1983 Effect of heme on Bacteroides distasonis catalase and aerotolerance *Journal of bacteriology* **156** 1012-8

[12] Beveridge T J 1999 Structures of gram-negative cell walls and their derived membrane vesicles *Journal of bacteriology* **181** 4725-33

[13] Siddique M N, Faizan M, Riyajuddin S, Tripathi P, Ahmad S and Ghosh K 2021 Intrinsic structural distortion assisted optical and magnetic properties of orthorhombic rare-earth perovskite La1-xEuxCrO3: Effect of t-e hybridization *Journal of Alloys and Compounds* **850** 156748

[14] Keyer K, Gort A S and Imlay J A 1995 Superoxide and the production of oxidative DNA damage *Journal of bacteriology* **177** 6782-90

[15] Sonohara R, Muramatsu N, Ohshima H and Kondo T 1995 Difference in surface properties between Escherichia coli and Staphylococcus aureus as revealed by electrophoretic mobility measurements *Biophysical chemistry* **55** 273-7

[16] Singh A and Dubey A K 2018 Various biomaterials and techniques for improving antibacterial response *ACS Applied Bio Materials* **1** 3-20

[17] Swain S, Padhy R N and Rautray T R 2020 Polarized piezoelectric bioceramic composites exhibit antibacterial activity *Materials Chemistry and Physics* **239** 122002

[18] Kumar S, Vaish R and Powar S 2018 Surface-selective bactericidal effect of poled ferroelectric materials *Journal of Applied Physics* **124** 014901

[19] Singh A, Reshma K and Dubey A K 2020 Combined effect of surface polarization and ZnO addition on antibacterial and cellular response of Hydroxyapatite-ZnO composites *Materials Science and Engineering: C* **107** 110363

[20] Dubey A K and Basu B 2014 Pulsed electrical stimulation and surface charge induced cell growth on multistage spark plasma sintered hydroxyapatite-barium titanate piezobiocomposite *Journal of the American Ceramic Society* **97** 481-9

[21] Harkes G, Feijen J and Dankert J 1991 Adhesion of Escherichia coli on to a series of poly(methacrylates) differing in charge and hydrophobicity *Biomaterials* **12** 853-60

[22] Kodjikian L, Burillon C, Roques C, Pellon G, Freney J and Renaud F N 2003 Bacterial adherence of Staphylococcus epidermidis to intraocular lenses: a bioluminescence and scanning electron microscopy study *Investigative ophthalmology & visual science* **44** 4388-94

[23] Okada A, Nikaido T, Ikeda M, Okada K, Yamauchi J, Foxton R M, Sawada H, Tagami J and Matin K 2008 Inhibition of Biofilm Formation using Newly Developed Coating Materials with Self-cleaning Properties *Dental Materials Journal* **27** 565-72

[24] Khare D, Singh A and Dubey A K 2021 Influence of Na and K contents on the antibacterial response of piezoelectric biocompatible NaxK1-xNbO3 (x= 0.2–0.8) *Materials Today Communications* **27** 102317

[25] Ehrensberger M T, Tobias M E, Nodzo S R, Hansen L A, Luke-Marshall N R, Cole R F, Wild L M and Campagnari A A 2015 Cathodic voltage-controlled electrical stimulation of titanium implants as treatment for methicillin-resistant Staphylococcus aureus periprosthetic infections *Biomaterials* **41** 97-105

[26] Xie Y and Yang L 2016 Calcium and magnesium ions are membrane-active against stationary-phase Staphylococcus aureus with high specificity *Scientific reports* **6** 20628

[27] Jangra S L, Stalin K, Dilbaghi N, Kumar S, Tawale J, Singh S P and Pasricha R 2012 Antimicrobial activity of zirconia (ZrO2) nanoparticles and zirconium complexes *Journal of nanoscience and nanotechnology* **12** 7105-12

[28] Kim S-H, Lee H-S, Ryu D-S, Choi S-J and Lee D-S 2011 Antibacterial activity of silver-nanoparticles against Staphylococcus aureus and Escherichia coli *Microbiology and Biotechnology Letters* **39** 77-85